AIP | Applied Physics Letters

Long electron spin coherence in ionimplanted GaN: The role of localization

J. H. Buß, J. Rudolph, S. Shvarkov, H. Hardtdegen, A. D. Wieck, and D. Hägele

Citation: Applied Physics Letters **102**, 192102 (2013); doi: 10.1063/1.4804558
View online: http://dx.doi.org/10.1063/1.4804558
View Table of Contents: http://scitation.aip.org/content/aip/journal/apl/102/19?ver=pdfcov
Published by the AIP Publishing

Long electron spin coherence in ion-implanted GaN: The role of localization

J. H. Buß,[1] J. Rudolph,[1] S. Shvarkov,[2] H. Hardtdegen,[3] A. D. Wieck,[2] and D. Hägele[1]
[1]*Arbeitsgruppe Spektroskopie der kondensierten Materie, Ruhr-Universität Bochum, Universitätsstraße 150, D-44780 Bochum, Germany*
[2]*Angewandte Festkörperphysik, Ruhr-Universität Bochum, Universitätsstraße 150, D-44780 Bochum, Germany*
[3]*Forschungszentrum Jülich, Peter Grünberg Institut PGI 9, D-52425 Jülich, Germany*

(Received 28 March 2013; accepted 26 April 2013; published online 13 May 2013)

The impact of Ga and Au ion implantation on the electron spin dynamics in bulk wurtzite GaN is studied by time-resolved Kerr-rotation spectroscopy. The spin relaxation time increases strongly by up to a factor of 20 for increasing implantation doses. This drastic increase is caused by a transition from delocalized to localized electrons. We find a characteristic change in the magnetic field dependence of spin relaxation that can be used as a sensitive probe for the degree of localization. [http://dx.doi.org/10.1063/1.4804558]

The electron spin dynamics in semiconductors is governed by the multifarious interplay of numerous parameters.[1,2] Besides tunable extrinsic parameters like temperature or external magnetic fields, the intrinsic material properties like crystal symmetry or strength of the spin orbit coupling (SOC) play a key role. In addition to these properties of the ideal material, also the disorder potential in a real semiconductor structure has strong influence on the spin dynamics as it modifies momentum scattering of delocalized electrons or even leads to localization of carriers. Despite its importance, the influence of disorder on the electron spin dynamics has only rarely been studied systematically by changing the electron density and thus the degree of localization for a fixed disorder potential.[3,4] The disorder potential itself can, however, also be modified by implanting ions into the semiconductor where the implanted ions and the implantation damage strongly influence the disorder potential. In addition to these fundamental aspects, the electron spin dynamics in ion-implanted semiconductors is also highly relevant for the development of spintronics as a spin based electronics. Vacancies as typical implantation defects were for example proposed as spin filters[5] or predicted to cause ferromagnetism in wide-gap group III nitrides.[6] In this context, especially GaN has attracted strong interest as a possible ferromagnetic semiconductor after various experimental reports on ferromagnetism upon ion implantation.[7–10] Here, we experimentally investigate the electron spin dynamics in bulk wurtzite GaN implanted with Ga and Au ions by time-resolved magneto-optical Kerr-rotation (TRKR) spectroscopy.

The GaN sample under investigation was a 1.8 μm thick GaN layer with a typical n-type doping level of $n_D \approx 5 \times 10^{16}\,\mathrm{cm}^{-3}$, grown by metal-organic chemical vapor deposition (MOCVD) on a sapphire substrate. Six $1 \times 1\,\mathrm{mm}^2$ wide regions were implanted with different Ga doses ranging from $1 \times 10^{11}\,\mathrm{cm}^{-2}$ to $1 \times 10^{13}\,\mathrm{cm}^{-2}$. The implantation was carried out at room-temperature using a focused ion beam (FIB) implanter with Ga^+ ions at an implantation energy of 100 keV. The implanted doses correspond to average Ga densities from $n_{\mathrm{Ga}} = 1 \times 10^{16}\,\mathrm{cm}^{-3}$ to $1 \times 10^{18}\,\mathrm{cm}^{-3}$ as estimated for the projected stopping range of 100 nm resulting from SRIM simulations.[11] We note that even the highest implanted Ga density does virtually not change the stoichiometry of the GaN matrix. For comparison, four $1 \times 1\,\mathrm{mm}^2$ wide regions were implanted with Au^{2+} ions at an implantation energy of 200 keV and doses ranging from $5 \times 10^{10}\,\mathrm{cm}^{-2}$ to $1 \times 10^{12}\,\mathrm{cm}^{-2}$, corresponding to average densities $n_{\mathrm{Au}} = 6.7 \times 10^{15}\,\mathrm{cm}^{-3}$ to $1.3 \times 10^{17}\,\mathrm{cm}^{-3}$ for the projected stopping range of 75 nm. The sample was not annealed after implantation to preserve the implantation damage.

In the following, we will first focus on the effect of Ga implantation. The implanted regions were initially characterized by time-resolved photoluminescence (PL) measurements using the frequency-doubled output of a fs-Ti:Sapphire laser with an energy of 3.55 eV and 10 mW average power for excitation and a synchroscan streak-camera for detection. The PL shows for all implantation densities a fast decay (see exemplarily the PL transient in the inset of Fig. 1). The radiative lifetime slightly decreases from $\tau_r \approx 40$ ps for the unimplanted GaN to $\tau_r \approx 30$ ps for the highest implantation dose due to the increasing density of defects with short capture times. The intensity of the time-integrated PL strongly decreases for increasing implantation density, and is almost completely quenched for the highest implanted Ga density (see Fig. 1). This typical drop of the PL intensity is caused by the increasing implantation damage with the creation of nonradiative recombination centers.[12]

We next performed TRKR experiments to investigate the impact of the implantation damage on the electron spin dynamics. For these measurements, the frequency-doubled output of a modelocked Ti:Sapphire laser with a repetition rate of 80 MHz was split into pump and probe pulses. The circularly polarized pump pulse created a spin polarized electron ensemble in the sample. The time evolution of the spin polarization was monitored via the Kerr rotation of the linearly polarized probe pulse which was time delayed by a mechanical delay line. A balanced photoreceiver with cascaded lock-in amplifier technique was used for detection of the Kerr rotation, with a fast 50 kHz polarization modulation of the pump beam via a photoelastic modulator and a much slower intensity modulation of the probe beam. The average power of pump and probe beam was 10 mW and 1 mW,

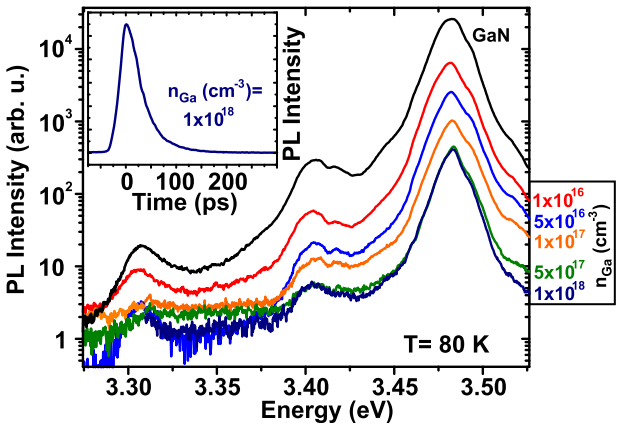

FIG. 1. Time-integrated PL spectra for different Ga implantation densities n_{Ga}. The inset shows the spectrally integrated PL transient for the highest implanted Ga density $n_{Ga} = 1 \times 10^{18}\,cm^{-3}$.

respectively, at an energy of 3.48 eV, corresponding to an estimated density $n_{exc} \approx 1 \times 10^{16}\,cm^{-3}$ of photoexcited carriers within the pump focus spot diameter of 100 μm. The sample was mounted in a cold-finger cryostat at a temperature of $T = 80$ K, and an external magnetic field B_{ext} was applied in the sample plane.

Figure 2 shows normalized TRKR transients for different Ga implantation densities n_{Ga}. The transients show oscillations due to the electrons' spin Larmor precession around the external magnetic field and a temporal decay due to the electron spin relaxation. The corresponding spin relaxation time τ_s was obtained by exponential decay fits of the form $[A_1\exp(-t/\tau_c) + A_2]\exp(-t/\tau_{s,0})$ to the zero-field ($B_{ext} = 0$) transients, and from damped cosine fits $[A_1\exp(-t/\tau_c) + A_2]\exp(-t/\tau_{s,B})\cos[\omega_L(t - t_0)]$ to the transients for $B_{ext} > 0$ where τ_c is a carrier lifetime and $\omega_L = g\mu_B B_{ext}/\hbar$ is the Larmor precession frequency. From the $\omega_L(B_{ext})$ dependence, a Landé-g factor $g = 1.95$ was obtained for the as grown GaN and for all implantation densities, in good agreement with the literature value for GaN.[13] The spin relaxation times τ_s for zero magnetic field (filled symbols) and a fixed magnetic field $B_{ext} = 0.24$ T (open symbols) are plotted in Fig. 3(a) as a function of the implantation density n_{Ga}. While

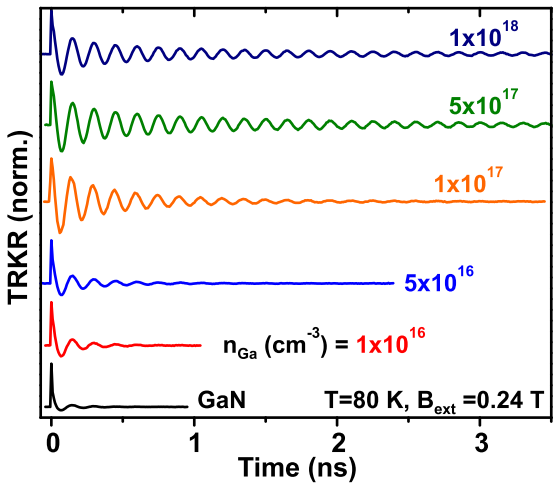

FIG. 2. Normalized TRKR transients for different Ga implantation densities n_{Ga}.

the spin relaxation times increase only moderately for low implantation densities, they show a drastic increase around the intermediate implantation density $n_{Ga} = 1 \times 10^{17}\,cm^{-3}$, before they saturate for even higher Ga doses. This pronounced density dependence is accompanied by a systematic change in the magnetic field dependence of spin relaxation as indicated by the ratio $\beta = \tau_{s,0}/\tau_{s,B}$ of the zero-field spin relaxation time $\tau_{s,0}$ to the spin relaxation time $\tau_{s,B}$ for $B_{ext} = 0.24$ T [see Fig. 3(b)]. In the following, we will show that the observed implantation density dependence of the spin relaxation time is caused by the transition from delocalized to localized electrons, and that the ratio β is a sensitive probe for localization.

We start by discussing the two limiting cases of spin relaxation of free electrons and of localized electrons with special emphasis on their magnetic field dependence. Free electrons are subject to Dyakonov-Perel[14] (DP) spin relaxation in n-GaN.[15–18] Spin-orbit coupling causes a conduction band spin splitting which acts like an effective, momentum dependent magnetic field $\Omega(\mathbf{k})$ on the electrons' spins. Random momentum scattering leads to a fluctuating effective magnetic field, resulting in spin dephasing of the electron ensemble. In the most simplistic approach to DP relaxation in the motional narrowing regime, the tensor of spin relaxation rates is given by[19]

$$\gamma_{ij} = \frac{1}{2}(\delta_{ij}\langle\Omega^2\rangle - \langle\Omega_i\Omega_j\rangle)\tau_p \qquad (1)$$

with the momentum scattering time τ_p and $\langle\ldots\rangle$ denoting averaging over the electrons' momentum distribution. More frequent momentum scattering leads therefore to longer spin relaxation times. The effective magnetic field in bulk wurtzite GaN is given by[20]

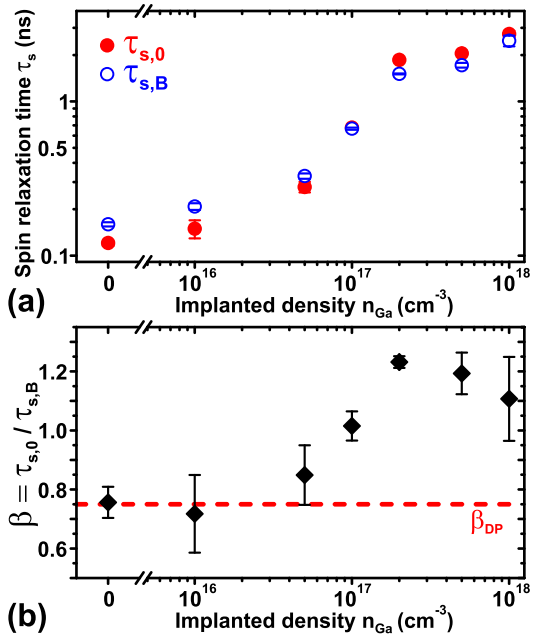

FIG. 3. (a) Spin relaxation times $\tau_{s,0}$ (filled symbols) and $\tau_{s,B}$ (open symbols) for zero magnetic field and $B_{ext} = 0.24$ T, respectively, as a function of the Ga implantation density n_{Ga}. (b) Ratio $\beta = \tau_{s,0}/\tau_{s,B}$ of the spin relaxation times. The dashed line indicates the value $\beta_{DP} = 0.75$ for DP relaxation.

$$\Omega(\mathbf{k}) = \frac{2}{\hbar}\left(\gamma_e(bk_z^2 - k_{||}^2) + \alpha_e\right)(k_y, -k_x, 0) \qquad (2)$$

with $z|||[0001]$ (c-axis), $x|||[11\bar{2}0]$, $y|||[1\bar{1}00]$, $k_{||}^2 = k_x^2 + k_y^2$, γ_e and b as Dresselhaus parameters and α_e as the Rashba coefficient. The anisotropic effective magnetic field leads according to Eq. (1) to an anisotropic spin relaxation tensor as elaborated in Ref. 15. This anisotropy manifests itself in a characteristic sudden rise from the spin relaxation time $\tau_{s,0}$ for zero magnetic field to $\tau_{s,B} = \frac{4}{3}\tau_{s,0}$ if an external magnetic field is applied. Therefore, a ratio $\beta_{\mathrm{DP}} = 0.75$ follows for DP relaxation of free, delocalized electrons in GaN.

In the other limiting case of spin relaxation of localized electrons, the DP mechanism is switched off since the bound states have zero average wave vectors. Instead, spin dephasing times are usually limited by spin-orbit interactions or hyperfine interaction with nuclear spins.[21,22] The spin dephasing due to the hyperfine interaction is isotropic, since it is dominated by the Fermi contact interaction.[23] The corresponding spin dephasing time due to the hyperfine interaction can be approximated by[24,25]

$$\tau_{s,\mathrm{nuc}} = \hbar\sqrt{\frac{3N}{2\sum_i I_i(I_i+1)A_i^2 y_i}}, \qquad (3)$$

where N is the number of nuclei overlapping with the electron wavefunction, A_i is the hyperfine constant, I_i the nuclear spin and y_i the abundance of isotope i. A spin dephasing time $\tau_{s,\mathrm{nuc}} \approx 1.8$ ns is estimated, in approximate agreement with the experiment.[26,30] An additional contribution to spin dephasing of localized electrons can arise in magnetic fields from a distribution Δg of the electron g factor.[27] It leads to a spread $\Delta\omega_L = \Delta g \mu_B B/\hbar$ in the Larmor precession frequency, resulting in an inhomogeneous dephasing of the electron spin. The corresponding magnetic field dependence

$$\tau_{s,\mathrm{loc}}(B_{\mathrm{ext}}) = 1\Big/\sqrt{(1/\tau_{s,\mathrm{loc}}(0))^2 + (\Delta g \mu_B B_{\mathrm{ext}}/\hbar)^2} \qquad (4)$$

with a $\tau_{s,\mathrm{loc}} \propto 1/B_{\mathrm{ext}}$ dependence for large B_{ext} is well-known for localized electrons in such different systems as quantum dots,[25] potential fluctuations in quantum wells[3] or donor-bound electrons.[22] The regime of localized electrons is correspondingly characterized by a ratio $\beta_{\mathrm{loc}} > 1$.

In the experiment, we find purely DP dominated spin relaxation of free, delocalized electrons for the unimplanted GaN and the lowest implantation density $n_{\mathrm{Ga}} = 1 \times 10^{16}\,\mathrm{cm}^{-3}$, as evidenced by a ratio $\beta \approx 0.75$ [cf. Fig. 3(b)] and the characteristic magnetic field dependence with a sudden increase of the spin relaxation time from $\tau_{s,0}$ to $\tau_{s,B} = \frac{4}{3}\tau_{s,0}$ [see Figs. 4(a) and 4(b)]. The spin relaxation times are found in good agreement with similar, unimplanted GaN samples.[15–17]

For the highest implantation densities $n_{\mathrm{Ga}} \geq 2 \times 10^{17}\,\mathrm{cm}^{-3}$, the spin relaxation is in contrast characteristic for localized electrons, with a constant spin relaxation time compatible with nuclear hyperfine relaxation as shown above and a typical magnetic field dependence possibly due to g factor variations [see Figs. 3(a), 4(a), and 4(c)]. A fit to the magnetic field dependence according to Eq. (4) gives good

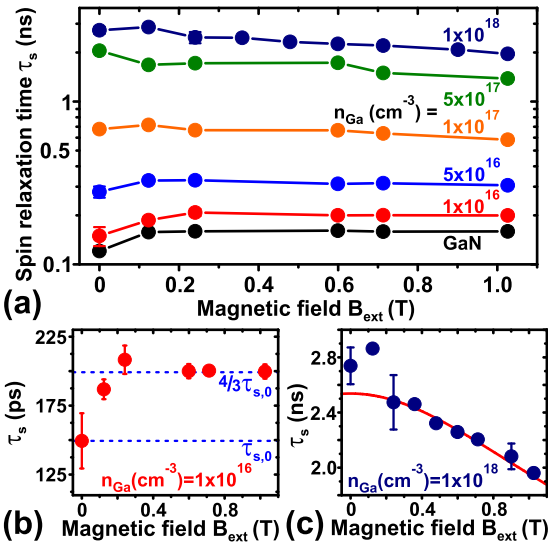

FIG. 4. (a) Magnetic field dependence of the spin relaxation time for different Ga implantation densities. (b) Magnetic field dependence of the spin relaxation time τ_s for $n_{\mathrm{Ga}} = 1 \times 10^{16}\,\mathrm{cm}^{-3}$. The dashed lines mark the zero-field value $\tau_{s,0}$ and the value $\tau_{s,B} = 4/3\tau_{s,0}$ predicted by DP theory. (c) Magnetic field dependence of τ_s for the highest implanted Ga density $n_{\mathrm{Ga}} = 1 \times 10^{18}\,\mathrm{cm}^{-3}$. The solid line is a fit to Eq. (4).

agreement for the highest implanted density $n_{\mathrm{Ga}} \geq 1 \times 10^{18}\,\mathrm{cm}^{-3}$ and $B_{\mathrm{ext}} > 0.2$ T [see Fig. 4(c)]. We note that the required variation of the Landé-g factor $\Delta g = 0.0037$ corresponds to only 0.2% variation of g. Responsible for the observed localization is defects created during implantation, where, e.g., the N vacancy is a donor state.[28]

The strongly increasing spin relaxation time in the intermediate regime reflects the transition from delocalized to localized electrons. Fast spin exchange between the ensemble of free and localized electrons leads to the observation of a single relaxation time.[21,29] The increasing contribution of the slowly relaxing localized electrons leads to the observed increase of spin relaxation time with implantation density. The magnetic field dependence shows a corresponding transition from the characteristic anisotropic DP magnetic field dependence over a flattening for $n_{\mathrm{Ga}} = 1 \times 10^{17}\,\mathrm{cm}^{-3}$ to the $\tau_s \propto 1/B_{\mathrm{ext}}$ dependence of localized electrons [see Fig. 4(c)]. This interpretation is corroborated by measurements at room temperature where we find a recovery of the anisotropic relaxation and ratios β close to $\beta_{\mathrm{DP}} = 0.75$ for all implanted densities as a consequence of the smaller degree of localization at room temperature (not shown). We note that increasing spin lifetimes for increasing implantation dose are also generally predicted within DP theory for delocalized electrons as a consequence of increasing momentum scattering [see Eq. (1)]. This interpretation would, however, predict a persistence of the spin relaxation anisotropy, in contrast to the experimental findings. We therefore rule out the explanation of the increasing spin relaxation times via the DP mechanism.

For comparison, we also measured the spin relaxation times after implantation of Au ions (see Fig. 5). The spin relaxation times and the ratio β show a very similar over-all behavior as for Ga implantation. The drastic increase of spin relaxation times starts, however, for a lower density $n_{\mathrm{Au}} = 5 \times 10^{16}\,\mathrm{cm}^{-3}$, as can be expected from the higher

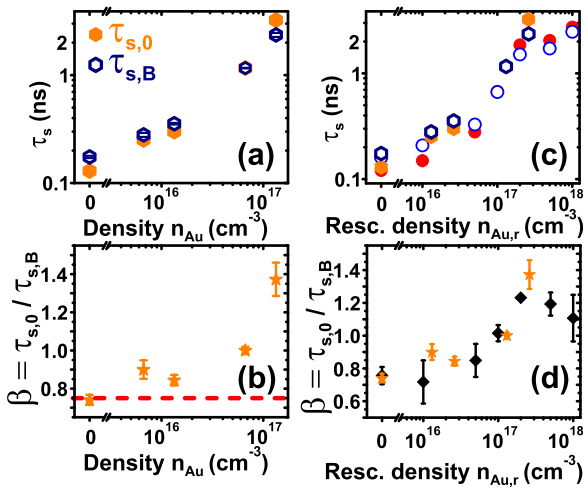

FIG. 5. (a) Spin relaxation times $\tau_{s,0}$ (filled symbols) and $\tau_{s,B}$ (open symbols) for zero magnetic field and $B_{ext} = 0.24$ T, respectively, as a function of the Au implantation density n_{Au}. (b) Ratio $\beta = \tau_{s,0}/\tau_{s,B}$ of the spin relaxation times. The dashed line indicates the value $\beta_{DP} = 0.75$ for DP relaxation. (c) Spin relaxation times and (d) ratio β for the rescaled implanted density $n_{Au,r} = N_{dam} n_{Au}$ in comparison to the values for Ga implantation.

mass of Au ions and the accordingly higher implantation damage. We estimated the implantation damage by SRIM simulations of the number $N_{vac,Au/Ga}$ of vacancies per Au and Ga ions. Rescaling the implanted Au density by the ratio $N_{dam} = N_{vac,Au}/N_{vac,Ga} = 1.96$ obtained from the simulations gives good agreement between the density dependence for Ga and Au ions [see Figs. 5(c) and 5(d)], suggesting that the defects dominating the localization are the same, independent of the implanted ion species.

In conclusion, the influence of Ga and Au ion implantation on the electron spin dynamics in bulk GaN was studied. Independent of the implanted ion species, we find a strong increase of the spin relaxation time by up to a factor of 20 with increasing implantation dose that is caused by increasing carrier localization. The corresponding magnetic field dependence of spin relaxation shows a transition from the anisotropic relaxation of delocalized electrons to isotropic relaxation of localized carriers, which makes it a sensitive probe for localization.

We gratefully acknowledge financial support by the German Science Foundation (DFG priority program 1285 "Semiconductor Spintronics").

[1]*Spin Physics in Semiconductors*, edited by M. I. Dyakonov (Springer-Verlag, Berlin, 2008).
[2]M. W. Wu, J. H. Jiang, and M. Q. Weng, Phys. Rep. **493**, 61 (2010).
[3]Z. Chen, S. G. Carter, R. Bratschitsch, P. Dawson, and S. T. Cundiff, Nature Phys. **3**, 265 (2007).
[4]Z. Chen, S. G. Carter, R. Bratschitsch, and S. T. Cundiff, Physica E **42**, 1803 (2010).
[5]X. J. Wang, I. A. Buyanova, F. Zhao, D. Lagarde, A. Balocchi, X. Marie, C. W. Tu, J. C. Harmand, and W. M. Chen, Nature Mater. **8**, 198 (2009).
[6]P. Dev, Y. Xue, and P. Zhang, Phys. Rev. Lett. **100**, 117204 (2008).
[7]S. Dhar, T. Kammermeier, A. Ney, L. Pérez, K. H. Ploog, A. Melnikov, and A. D. Wieck, Appl. Phys. Lett. **89**, 062503 (2006).
[8]R. P. Davies, B. P. Gila, C. R. Abernathy, S. J. Pearton, and C. J. Stanton, Appl. Phys. Lett. **96**, 212502 (2010).
[9]G. Talut, H. Reuther, S. Zhou, K. Potzger, F. Eichhorn, and F. Stromberg, J. Appl. Phys. **102**, 083909 (2007).
[10]J.-H. Lee, I.-H. Choi, S. Shin, S. Lee, J. Lee, C. Whang, S.-C. Lee, K.-R. Lee, J.-H. Baek, K. H. Chae, and J. Song, Appl. Phys. Lett. **90**, 032504 (2007).
[11]J. F. Ziegler, M. D. Ziegler, and J. P. Biersack, Nucl. Instrum. Methods Phys. Res. B **268**, 1818 (2010).
[12]C. Ronning, E. P. Carlson, and R. F. Davis, Phys. Rep. **351**, 349 (2001).
[13]W. E. Carlos, J. A. Freitas, Jr., M. Asif Khan, D. T. Olson, and J. N. Kuznia, Phys. Rev. B **48**, 17878 (1993).
[14]M. I. Dyakonov and V. I. Perel, Sov. Phys. Solid State **13**, 3023 (1972).
[15]J. H. Buß, J. Rudolph, F. Natali, F. Semond, and D. Hägele, Appl. Phys. Lett. **95**, 192107 (2009).
[16]J. H. Buß, J. Rudolph, F. Natali, F. Semond, and D. Hägele, Phys. Rev. B **81**, 155216 (2010).
[17]J. H. Buß, J. Rudolph, S. Starosielec, A. Schaefer, F. Semond, Y. Cordier, A. D. Wieck, and D. Hägele, Phys. Rev. B **84**, 153202 (2011).
[18]J. H. Buß, J. Rudolph, T. Schupp, D. J. As, K. Lischka, and D. Hägele, Appl. Phys. Lett. **97**, 062101 (2010).
[19]D. Hägele, S. Döhrmann, J. Rudolph, and M. Oestreich, Adv. Solid State Phys. **45**, 253 (2005).
[20]J. Y. Fu and M. W. Wu, J. Appl. Phys. **104**, 093712 (2008).
[21]K. V. Kavokin, Semicond. Sci. Technol. **23**, 114009 (2008).
[22]A. Greilich, A. Pawlis, F. Liu, O. A. Yugov, D. R. Yakovlev, K. Lischka, Y. Yamamoto, and M. Bayer, Phys. Rev. B **85**, 121303 (2012).
[23]A. M. Stoneham, *Theory of Defects in Solids* (Clarendon Press, Oxford, 1975).
[24]I. A. Merkulov, A. L. Efros, and M. Rosen, Phys. Rev. B **65**, 205309 (2002).
[25]M. Syperek, D. R. Yakovlev, I. A. Yugova, J. Misiewicz, I. V. Sedova, S. V. Sorokin, A. A. Toropov, S. V. Ivanov, and M. Bayer, Phys. Rev. B **84**, 085304 (2011).
[26]The number N of nuclei was estimated by the ratio of the electron localization volume to the unit cell volume, assuming a volume $V_e = 4/3\pi a_e^3$ for the localized electron wavefunction with a modified Bohr radius $a_e = 2\varepsilon_{GaN}/(m^*/m_e)a_H$. An averaged value $A = 45\,\mu$eV was used for the hyperfine constants. See also Ref. 30.
[27]J. A. Gupta, D. D. Awschalom, X. Peng, and A. P. Alivisatos, Phys. Rev. B **59**, R10421 (1999).
[28]D. C. Look, D. C. Reynolds, J. W. Hemsky, J. R. Sizelove, R. L. Jones, and R. J. Molnar, Phys. Rev. Lett. **79**, 2273 (1997).
[29]D. Paget, Phys. Rev. B **24**, 3776 (1981).
[30]M. Q. Weng, Y. Y. Wang, and M. W. Wu, Phys. Rev. B **79**, 155309 (2009).